

Orbital diffusion, polarization and swapping in centrosymmetric metals

Xiaobai Ning^{1,2}, A. Pezo^{1,3}, Kyoung-Whan Kim⁴, Weisheng Zhao², Kyung-Jin Lee⁵, and Aurélien Manchon^{1*}

¹*Aix-Marseille Univ, CNRS, CINaM, Marseille, France;* ²*Fert Beijing Institute,*

School of Integrated Circuit Science and Engineering,

National Key Laboratory of Spintronics, Beihang University,

Beijing, China; ³*Laboratoire Albert Fert, CNRS, Thales,*

Université Paris-Saclay, 91767, Palaiseau, France; ⁴*Department of Physics,*

Yonsei University, Seoul, Korea; ⁵*Department of Physics,*

Korea Advanced Institute of Science and Technology (KAIST), Daejeon 34141, Korea

We propose a general theory of charge, spin, and orbital diffusion based on Keldysh formalism. Our findings indicate that the diffusivity of orbital angular momentum in metals is much lower than that of spin or charge due to the strong orbital intermixing in crystals. Furthermore, our theory introduces the concept of “spin-orbit polarization” by which a pure orbital (spin) current induces a longitudinal spin (orbital) current, a process as efficient as spin polarization in ferromagnets. Finally, we find that orbital currents undergo momentum swapping, even in the absence of spin-orbit coupling. This theory establishes several key parameters for orbital transport of direct importance to experiments.

Introduction - The interconversion between charge and spin currents¹ is one of the central mechanisms of spintronics and possibly its most instrumental. This mechanism is at the source of spin-orbit torque² and charge currents induced by spin pumping³. At the core of these phenomena lies the spin-orbit interaction that couples the spin to the orbital angular momentum in high-Z materials (5d metals, topological materials etc.). In recent years, it has been proposed that the interconversion between charge and orbital currents, via orbital Hall^{4–6} and orbital Rashba effects^{7–9} for instance, might in fact be much more efficient than its spin counterpart because it arises from the orbital texture imposed by the crystal field rather than from spin-orbit coupling. Therefore, corresponding phenomena such as orbital torque^{10–13} and orbital magnetoresistance¹⁴ have been proposed and experimentally reported. In these experiments, the scenario is based on a two-step process: orbital Hall or Rashba effect takes place in a light metal and the resulting orbital current is converted into a spin signal once in the adjacent ferromagnet. Consequently, it is expected that the supposedly large charge-to-orbital conversion taking place in the low-Z metal compensates for the relatively low spin-orbit coupling of the ferromagnet, which seems to be confirmed by the experiments^{11,12,14–17}.

An important rationale behind the promotion of orbitronics is twofold. First, as mentioned above, since orbital transport is governed by the crystal field, orbital Hall and Rashba effects do not necessitate spin-orbit coupling and occur in low-Z metals (e.g., 3d metals). Second, orbital currents are expected to propagate over reasonable distances (~ 10 nm) because they are immune to spin scattering, which seems confirmed by recent experiments^{16–19}. On the other hand, several questions remain open. To start with, as observed by Ref. 4, the

atomic orbital moment is never a good quantum number and therefore it remains unclear how it diffuses from one metal to another. Recent phenomenological models of orbital diffusion have been recently proposed^{15,20} but lack quantitative predictability by overlooking microscopic details. In addition, several recent works have pointed out that the orbital moment arises not only from intra-atomic spherical harmonics (p , d) but also possesses substantial inter-atomic contribution^{21–23}. Understanding the way orbital currents and densities propagate in metals and accumulate at interfaces requires determining transport coefficients such as orbital conductivity or diffusivity, as well as the ability to interconvert spin currents into orbital currents via spin-orbit coupling. Indeed, when injecting an orbital density $\mathbf{l} = \langle \mathbf{L} \rangle$ in a metal, it diffuses and produces an orbital current $\mathcal{J}_l = -D_l \partial_r \mathbf{l}_r$, D_l being the orbital diffusion coefficient (typically a tensor). In the presence of spin-orbit coupling $\xi_{so} \hat{\sigma} \cdot \hat{\mathbf{L}}$, this orbital current can convert into a spin current \mathcal{J}_s .

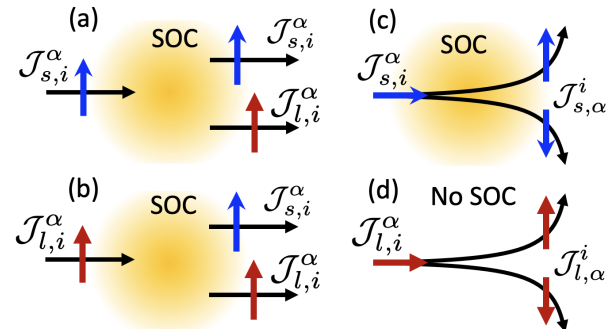


FIG. 1. (Color online) Spin and orbit interconversion mechanisms: (a) spin-to-orbit polarization and (b) orbit-to-spin polarization mediated by spin-orbit coupling. (c) Spin and (d) orbital swapping. The former requires spin-orbit coupling whereas the latter occurs even without it.

* aurelien.manchon@univ-amu.fr

In this Letter, we derive a theory of spin and orbital diffusion in metals and uncover several mechanisms governing orbital torque and magnetoresistance phenomena, illustrated in Fig. 1. First, we find that whereas charge and spin diffusion are of about the same order of magnitude, the orbital diffusion is much lower. This is due to the fact that the orbital moment is never a good quantum number in crystals (rotational invariance is broken). Second, we find that in the presence of spin-orbit coupling, an orbital current is systematically accompanied by a spin current that is collinear to it (and vice versa) [Fig. 1(a,b)]. This "spin-orbit polarization" can be sizable, comparable to spin polarization in 3d ferromagnets. Finally, the third class of effects uncovered by our theory is the "angular momentum swapping", i.e., the interchange between the propagation direction and angular momentum direction upon scattering [Fig. 1(c,d)]. Whereas spin swapping was predicted by Lifshits and Dyakonov²⁴ in the presence of spin-orbit coupling, orbital swapping arises naturally even without it. When turning on spin-orbit coupling, not only spin swapping emerges, but also spin-to-orbit and orbit-to-spin swapping.

Theory - The objective of the present theory is to determine the diffusive current induced by a gradient of particle density, $\mathcal{J} = -\mathcal{D}\partial_{\mathbf{r}}\rho$. In this expression, \mathcal{J} can be the charge current J_c , or the spin (orbital) current $\mathcal{J}_{s(l)}$, whereas ρ can be the charge density ρ_c , or the spin (orbital) density $\mathbf{s}(\mathbf{l})$. In the language of non-equilibrium Green's function, the particle current density is obtained by computing the quantum statistical expectation value of the trace of the particle current operator \hat{j} taken over the lesser Green's function $G^<$,

$$\mathcal{J} = \int \frac{d^3\mathbf{k}}{(2\pi)^3} \int \frac{d\varepsilon}{2i\pi} \text{Tr} [\hat{j} G^<]. \quad (1)$$

The philosophy of the present theory is to express the lesser Green's function to the first order in the density gradient $\partial_{\mathbf{r}}\rho$. We start from the Keldysh-Dyson equation²⁵

$$G^< = G^R \otimes \Sigma^< \otimes G^A, \quad (2)$$

where $G^< = G^<(\mathbf{r}, \mathbf{r}'; t, t')$ ($\Sigma^<$) is the lesser Green's function (self-energy), $G^{R(A)} = G^{R(A)}(\mathbf{r}, \mathbf{r}'; t, t')$ is the retarded (advanced) Green's function and \otimes is the convolution product on both time and space. In Eq. (2), we omitted the explicit time and space dependence for simplicity. In the linear response regime, we first express $G^<$ to the first order in spatial gradients using the Wigner transform (see, e.g., Ref. 26), i.e., we rewrite Eq. (2) in the frame of the center-of-mass, $(\mathbf{r}, \mathbf{r}'; t, t') \rightarrow (\mathbf{r} - \mathbf{r}', \mathbf{r}_c; t - t', t_c)$, with $(\mathbf{r}_c, t_c) = ((\mathbf{r} + \mathbf{r}')/2, (t + t')/2)$, Fourier transform the small space and time coordinates $(\mathbf{r} - \mathbf{r}', t - t') \rightarrow (\mathbf{k}, \omega)$, and expand Keldysh-Dyson equation to the first order in space and time gradients ($\partial_{\mathbf{r}_c}, \partial_{t_c}$). In the following, the subscript c is dropped for the sake of readability. Under the Wigner transform, the

convolution product becomes²⁶

$$A \otimes B = AB + \frac{i}{2} (\partial_{\mathbf{r}} A \partial_{\mathbf{k}} B - \partial_{\mathbf{k}} A \partial_{\mathbf{r}} B), \quad (3)$$

and finally, the part of the lesser Green's function that is linear in spatial gradient reads

$$\delta G^< = \frac{i}{2} (G_0^R \partial_{\mathbf{r}} \Sigma^< \partial_{\mathbf{k}} G_0^A - \partial_{\mathbf{k}} G_0^R \partial_{\mathbf{r}} \Sigma^< G_0^A). \quad (4)$$

Here $G_0^{R(A)} = (\hbar\omega - \mathcal{H}_0 \pm i\Gamma)$ is the unperturbed retarded (advanced) Green's function and \mathcal{H}_0 is the crystal Hamiltonian.

Since we are interested in the diffusion coefficients that connect angular momentum densities (odd under time-reversal \mathcal{T}) with angular momentum currents (even under \mathcal{T}), the diffusion coefficients in *nonmagnetic* materials are themselves odd under \mathcal{T} . The same is true for the charge diffusivity that connects the charge density (even under \mathcal{T}) with the charge current (odd under \mathcal{T}). As a result, the charge, spin, and orbital diffusion coefficients must be dissipative, proportional to the scattering time. In the language of quantum transport, these phenomena are driven by Fermi surface electrons akin to the charge conductivity. This is in stark contrast with the spin and orbital Hall diffusivities, which connect charge densities (even under \mathcal{T}) with spin and orbital currents (even under \mathcal{T}): they are even under \mathcal{T} , independent on scattering in the limit of weak disorder, and associated with the Berry curvature^{27,28}. Since we focus on angular momentum diffusion and spin-orbit interconversion, Eq. (4) is limited to transport at the Fermi level and disregards Fermi sea contributions. The present analysis applies to nonmagnetic materials and must be revised in the case of magnetic systems²⁹ as new terms are allowed.

Considering point-like impurities, $H_{\text{imp}} = \sum_i V_0 \delta(\mathbf{r} - \mathbf{R}_i)$, the lesser self-energy reads

$$\Sigma^< = \frac{1}{V} \sum_{i,j} \int \frac{d^3\mathbf{k}}{(2\pi)^3} V_0 G_{\mathbf{k}}^< V_0 e^{i\mathbf{k} \cdot (\mathbf{R}_i - \mathbf{R}_j)} = \frac{n_i V_0^2}{V} \langle G_{\mathbf{k}}^< \rangle. \quad (5)$$

Here, n_i is the impurity concentration and $\langle \dots \rangle = V \int \frac{d^3\mathbf{k}}{(2\pi)^3}$ stands for momentum integration over the Brillouin zone. Noting that $\partial_{\mathbf{k}} G_0^R = \hbar G_0^R \mathbf{v} G_0^R$, we obtain

$$\delta G_{\mathbf{k}}^< = i\hbar \frac{n_i V_0^2}{V} \text{Re} [G_0^R \partial_{\mathbf{r}} \langle G_{\mathbf{k}}^< \rangle G_0^A \mathbf{v} G_0^A]. \quad (6)$$

Inserting Eq. (6) into Eq. (1), we obtain the general expression of nonequilibrium properties induced by spatial gradients. Now, as argued above, diffusive effects are associated with Fermi surface electrons, which suggests $(1/V) \partial_{\mathbf{r}} \langle G_{\mathbf{k}}^< \rangle = 2i\pi \partial_{\mathbf{r}} \hat{\rho} \delta(\varepsilon - \varepsilon_F)$, $\hat{\rho}$ being the density matrix at Fermi level. As a result, the particle current density reads

$$\mathcal{J} = -\hbar n_i V_0^2 \text{Re} \text{Tr}_{\mathbf{k}} \left[\hat{j} \text{Im} [G_0^R \partial_{\mathbf{r}} \hat{\rho} G_0^A \mathbf{v} G_0^A] \right]_{\varepsilon_F}. \quad (7)$$

For the sake of compactness, we defined $\text{Tr}_{\mathbf{k}} = \int \frac{d^3 \mathbf{k}}{(2\pi)^3} \text{Tr}$. Equation (7) is the central result of this work and can be used to compute the diffusive charge, spin, and orbital currents induced by density gradients. For instance, substituting $\hat{\rho}$ by the charge density $\rho_c = -e\text{Tr}[\hat{\rho}]$, and the charge current operator $\hat{j} = -e\hat{\mathbf{v}}$, one obtains the charge diffusivity

$$\mathcal{D}_{ij} = \hbar n_i V_0^2 \text{Re} \text{Tr}_{\mathbf{k}} [\hat{v}_j \text{Im}[G_0^R G_0^A \hat{v}_i G_0^A]] . \quad (8)$$

The validity of Eq. (8) is readily assessed by comparing \mathcal{D}_{ij} with the conductivity σ_{ij} obtained from Kubo's formula²⁸. In the relaxation time approximation, $n_i V_0^2 = \Gamma / (\pi \mathcal{N}_F)$, where \mathcal{N}_F is the density of states at Fermi level and Γ is the disorder broadening. Using this relation, we confirm the Einstein relation $\mathcal{D}_{ij} = \sigma_{ij} / (e^2 \mathcal{N}_F)$ ²⁶. In the rest of this work, we express the spin and orbital diffusivity in the units of a conductivity $(e^2 \Gamma / (\pi n_i V_0^2)) \mathcal{D}_{ij}$, i.e., in $\Omega^{-1} \cdot m^{-1}$ rather than in $m^2 \cdot s^{-1}$.

To obtain the spin and orbital diffusivities, the respective densities are defined $\mathbf{s} = (\hbar/2) \text{Tr}[\hat{\sigma} \hat{\rho}]$ and $\mathbf{l} = \hbar \text{Tr}[\hat{\mathbf{L}} \hat{\rho}]$, $\hat{\sigma}$ and $\hat{\mathbf{L}}$ being the dimensionless spin and orbital operators. Therefore, substituting the current operator \hat{j} by either the spin current operator $\hat{j}_{s,j}^{\alpha} = (\hbar/4) \{\hat{v}_j, \hat{\sigma}_{\beta}\}$ or the orbital current operator $\hat{j}_{l,j}^{\beta} = (\hbar/2) \{\hat{v}_j, \hat{L}_{\beta}\}$ in Eq. (7), and $\partial_i \hat{\rho}$ by $\hat{\sigma}_{\alpha} \partial_i s_{\alpha}$ or $\hat{L}_{\alpha} \partial_i l_{\alpha}$, we obtain the general relation

$$\begin{pmatrix} \mathcal{J}_{s,j}^{\beta} \\ \mathcal{J}_{l,j}^{\beta} \end{pmatrix} = - \begin{pmatrix} \mathcal{D}_{s_{\alpha}i}^{s_{\beta}j} & \mathcal{D}_{l_{\alpha}i}^{s_{\beta}j} \\ \mathcal{D}_{s_{\alpha}i}^{l_{\beta}j} & \mathcal{D}_{l_{\alpha}i}^{l_{\beta}j} \end{pmatrix} \begin{pmatrix} \partial_i s_{\alpha} \\ \partial_i l_{\alpha} \end{pmatrix} \quad (9)$$

with the diffusion coefficients

$$\mathcal{D}_{s_{\alpha}i}^{s_{\beta}j} = 2n_i V_0^2 \text{Re} \text{Tr}_{\mathbf{k}} [\hat{j}_{s,j}^{\beta} \text{Im}[G_0^R \hat{\sigma}_{\alpha} G_0^A \hat{v}_i G_0^A]] , \quad (10)$$

$$\mathcal{D}_{l_{\alpha}i}^{l_{\beta}j} = n_i V_0^2 \text{Re} \text{Tr}_{\mathbf{k}} [\hat{j}_{l,j}^{\beta} \text{Im}[G_0^R \hat{L}_{\alpha} G_0^A \hat{v}_i G_0^A]] , \quad (11)$$

$$\mathcal{D}_{s_{\alpha}i}^{l_{\beta}j} = 2n_i V_0^2 \text{Re} \text{Tr}_{\mathbf{k}} [\hat{j}_{l,j}^{\beta} \text{Im}[G_0^R \hat{\sigma}_{\alpha} G_0^A \hat{v}_i G_0^A]] , \quad (12)$$

$$\mathcal{D}_{l_{\alpha}i}^{s_{\beta}j} = n_i V_0^2 \text{Re} \text{Tr}_{\mathbf{k}} [\hat{j}_{s,j}^{\beta} \text{Im}[G_0^R \hat{L}_{\alpha} G_0^A \hat{v}_i G_0^A]] . \quad (13)$$

$\mathcal{D}_{s_{\alpha}i}^{s_{\beta}j}$ represents a spin current $\mathcal{J}_{s,j}^{\beta}$ induced by the gradient of a spin density $\partial_i s_{\alpha}$, whereas $\mathcal{D}_{l_{\alpha}i}^{l_{\beta}j}$ represents an orbital current $\mathcal{J}_{l,j}^{\beta}$ induced by the gradient of an orbital density $\partial_i l_{\alpha}$. In addition, the diffusivities $\mathcal{D}_{s_{\alpha}i}^{l_{\beta}j}$ and $\mathcal{D}_{l_{\alpha}i}^{s_{\beta}j}$ represent the spin-to-orbital interconversion phenomena, i.e., spin-orbit polarization ($\alpha = \beta$) and spin-orbit swapping ($\alpha \neq \beta$).

Spin and orbital diffusion - To quantitatively estimate the magnitude of these effects in transition metals, we consider bcc crystalline structures with s, p, and d orbitals. An 18×18 tight-binding Hamiltonian is obtained using the two-center approximation of Slater-Koster parameterization³⁰. Parameters up to the second-nearest neighbor are applied for V ($\xi_{\text{so}} \approx 0$) and Ta

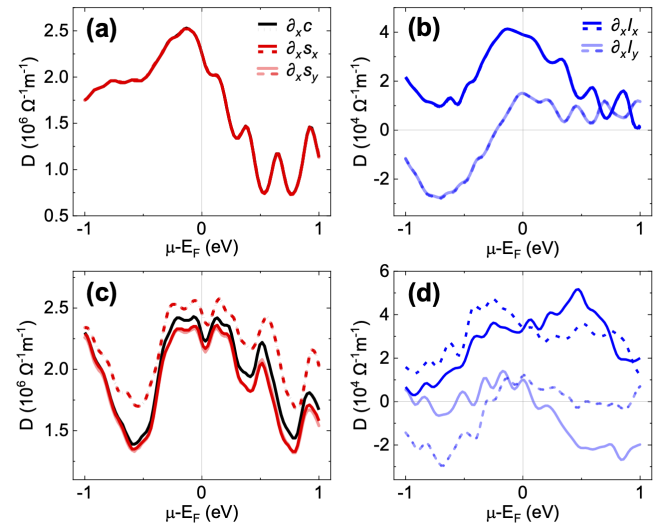


FIG. 2. (Color online) (a, c) Charge (black), spin (red) and (b, d) orbital diffusivities as a function of the energy, without (dashed lines) and with (solid lines) spin-orbit coupling, for (a, b) V and (c, d) Ta. The spin and orbital diffusivities are computed for both s_x, l_x (dark red, dark blue) and s_y, l_y components (light red, light blue). The orbital diffusivities are strongly anisotropic and two orders of magnitude smaller than the spin and charge diffusivities.

($\xi_{\text{so}} \neq 0$)³¹, which belong to Group V in the periodic table and consequently share similar electronic properties. Spin-orbit coupling is then added to the on-site energy³², with the operator $\hat{\mathbf{L}}$ defined in Ref. 33. The resulting band structures are benchmarked against density functional theory²⁶. To compute the transport properties, we set the disorder broadening to $\Gamma = 0.1$ eV and calculate the diffusion coefficients using a $50 \times 50 \times 50$ k -grid. A toy model featuring a bcc crystal with (p_x, p_y, p_z) orbitals is given in the Supplemental Materials²⁶ and qualitatively confirms the conclusions drawn from these realistic calculations.

We first compute the charge, spin, and orbital diffusivities in Fig. 2. Since the current diffuses in the same direction as the density gradient, $i = j$, its angular momentum is necessarily aligned with that of the density, $\alpha = \beta$. In vanadium, with vanishingly small spin-orbit coupling, we find that the charge diffusivity \mathcal{D}_{xx} and the spin diffusivities $\mathcal{D}_{s_{xx}}^{s_{xx}}, \mathcal{D}_{s_{yy}}^{s_{yy}} (= \mathcal{D}_{s_{zz}}^{s_{zz}})$ are all equal [Fig. 2(a)]. In tantalum [Fig. 2(b)], spin and charge diffusivities are slightly different due to the finite spin-orbit coupling, and $\mathcal{D}_{s_{xx}}^{s_{xx}} \approx \mathcal{D}_{s_{yy}}^{s_{yy}} (= \mathcal{D}_{s_{zz}}^{s_{zz}})$. Interestingly, as reported on Fig. 2(b,d), the orbital diffusivities $\mathcal{D}_{l_{xx}}^{l_{xx}} \neq \mathcal{D}_{l_{yy}}^{l_{yy}} (= \mathcal{D}_{l_{zz}}^{l_{zz}})$ are strongly anisotropic (dark and light blue lines) and, most importantly, are much smaller than the spin and charge diffusivities, which we attribute to the strong orbital mixing that naturally governs the band structure of our bcc crystal. In tantalum, spin-orbit coupling has a strong impact on the orbital diffusivity (dashed and solid lines). This can be understood qualitatively by the fact

that spin-orbit interaction couples the highly conductive spin channel with the weakly conductive orbital channel, thereby (slightly) reducing the spin diffusivity while enhancing the orbital one, as shown in Fig. 2(c,d).

The low orbital diffusivities reported here are not necessarily at odds with the decent orbital diffusion lengths (~ 10 nm) extracted from experiments in low-Z metals^{12,16–19}. Indeed, a comprehensive theory of orbital transport requires a microscopic modeling of orbital relaxation mechanisms, which remains out of the scope of the present work. Notice that in ferromagnets, spin dephasing severely limits the spin propagation, such that orbital diffusion naturally dominates^{12,13}. This effect is absent in nonmagnetic metals.

Spin-orbit polarization - The next question we wish to address is how much orbital current can one obtain upon injecting a spin current in a heavy metal. This mechanism underlies the phenomena of orbital torque and orbital magnetoresistance^{10–12,14–17} where a primary orbital current generated in a light metal is injected in a spin-orbit coupled material and converted into a spin current. To answer this question, we compute the so-called "spin-orbit polarization". Let us assume that a gradient of, say, spin density $\partial_i s_\alpha$ diffuses in the system. This gradient induces *both* spin and orbital currents, $\mathcal{J}_{s,i}^\alpha$ and $\mathcal{J}_{l,i}^\alpha$, producing a current of total angular momentum $\mathcal{J}_{t,i}^\alpha = \mathcal{J}_{l,i}^\alpha + \mathcal{J}_{s,i}^\alpha$. To quantify the relative proportion of spin and orbital currents, we define the spin-to-orbit polarization $\mathcal{P}_{l,i}^\alpha = |\mathcal{D}_{s_\alpha i}^{l_\alpha i}|/(|\mathcal{D}_{s_\alpha i}^{s_\alpha i}| + |\mathcal{D}_{s_\alpha i}^{l_\alpha i}|)$, and similarly, the orbit-to-spin polarization, $\mathcal{P}_{s,i}^\alpha = |\mathcal{D}_{l_\alpha i}^{s_\alpha i}|/(|\mathcal{D}_{l_\alpha i}^{l_\alpha i}| + |\mathcal{D}_{l_\alpha i}^{s_\alpha i}|)$. Since the sign of the diffusion coefficient varies across the band structure, only their absolute value enters the definition of the polarization.

The spin-to-orbit ($s_\alpha \rightarrow l_\alpha$) and orbit-to-spin ($l_\alpha \rightarrow s_\alpha$) longitudinal diffusivities in tantalum as well as the corresponding polarization are given in Fig. 3(a) and (b), respectively. In this material, spin-to-orbit (red line) and orbit-to-spin diffusion coefficients (blue lines) are anisotropic due to the presence of spin-orbit coupling and of similar magnitude. The orbital diffusivity being much smaller than the spin diffusivity (see Fig. 2), the orbit-to-spin polarization is generally larger than the spin-to-orbit polarization. As shown in Fig. 3(b), the polarization increases steadily with spin-orbit coupling, as expected, and saturates at large spin-orbit coupling strength. It is worth noting that the orbit-to-spin polarization is comparable to the spin polarization found in conventional 3d metal compounds (typically 50–70%). The sizable spin-orbit polarization given in Fig. 3(b) is a crucial ingredient for the orbital torque and magnetoresistance.

Spin, orbital and spin-orbit swapping - We finally consider the last class of effects, the spin and orbital swapping. For these effects, the directions of injection and collection are perpendicular to each other, as well as the direction of the incoming and outgoing (spin/orbit) polarization [see Fig. 1(c,d)]. The orbital diffusivity tensor

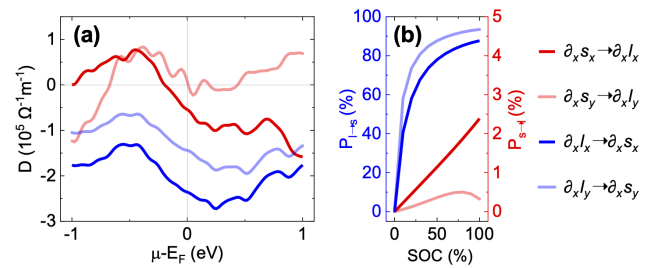


FIG. 3. (Color online) (a) Spin-to-orbit (red) and orbit-to-spin (blue) diffusivities as a function of the energy in tantalum. (b) Corresponding spin-orbit polarizations as a function of the spin-orbit coupling. 100% corresponds to the full spin-orbit coupling strength of tantalum.

has the following form

$$\begin{pmatrix} \mathcal{J}_{l,x}^x \\ \mathcal{J}_{l,x}^y \\ \mathcal{J}_{l,y}^x \\ \mathcal{J}_{l,y}^y \end{pmatrix} = - \begin{pmatrix} \mathcal{D}_{l_{xx}}^{l_{xx}} & 0 & 0 & \mathcal{D}_{l_{xy}}^{l_{xx}} \\ 0 & \mathcal{D}_{l_{yx}}^{l_{yx}} & \mathcal{D}_{l_{xy}}^{l_{yx}} & 0 \\ 0 & \mathcal{D}_{l_{xy}}^{l_{xy}} & \mathcal{D}_{l_{yy}}^{l_{xy}} & 0 \\ \mathcal{D}_{l_{xx}}^{l_{yy}} & 0 & 0 & \mathcal{D}_{l_{yy}}^{l_{yy}} \end{pmatrix} \begin{pmatrix} \partial_x l_x \\ \partial_x l_y \\ \partial_y l_x \\ \partial_y l_y \end{pmatrix}, \quad (14)$$

and Onsager reciprocity imposes that $\mathcal{D}_{l_{xy}}^{l_{yx}} = \mathcal{D}_{l_{yx}}^{l_{xy}}$ and $\mathcal{D}_{l_{xx}}^{l_{yy}} = \mathcal{D}_{l_{yy}}^{l_{xx}}$. Importantly, the orbital swapping does not necessitate spin-orbit coupling as it is solely governed by the orbital overlap (and hence the crystal field symmetry) of the crystal. These coefficients are reported in Fig. 4(a) for tantalum, without (dashed lines) and with (solid lines) spin-orbit coupling. Without spin-orbit coupling, only the orbital swapping is allowed (blue lines). Turning on the spin-orbit coupling triggers spin swapping²⁴ (red lines), whose diffusivity tensor has the same form as in Eq. (14). Figure 4(b) displays the spin (red) and orbital (blue) swapping efficiencies defined as $\eta_{s \rightarrow s} = |\mathcal{D}_{s_{xx}}^{s_{yy}}/\mathcal{D}_{s_{xx}}^{s_{xx}}|$ and $\eta_{l \rightarrow l} = |\mathcal{D}_{l_{xx}}^{l_{yy}}/\mathcal{D}_{l_{xx}}^{l_{xx}}|$, as a function of spin-orbit coupling, showing that orbital swapping is generally larger than spin swapping, which is reasonable given the minor role of spin-orbit coupling in the former.

In addition, spin-orbit coupling also enables the transfer between spin and orbital angular momenta that results in spin-to-orbit (red) and orbit-to-spin (blue) swapping, displayed in Fig. 4(c). The diffusivity tensor has the form

$$\begin{pmatrix} \mathcal{J}_{s,x}^x \\ \mathcal{J}_{s,x}^y \\ \mathcal{J}_{s,y}^x \\ \mathcal{J}_{s,y}^y \end{pmatrix} = - \begin{pmatrix} \mathcal{D}_{l_{xx}}^{s_{xx}} & 0 & 0 & \mathcal{D}_{l_{xy}}^{s_{xx}} \\ 0 & \mathcal{D}_{l_{yx}}^{s_{yy}} & \mathcal{D}_{l_{xy}}^{s_{yy}} & 0 \\ 0 & \mathcal{D}_{l_{xy}}^{s_{xy}} & \mathcal{D}_{l_{yy}}^{s_{xy}} & 0 \\ \mathcal{D}_{l_{xx}}^{s_{yy}} & 0 & 0 & \mathcal{D}_{l_{yy}}^{s_{yy}} \end{pmatrix} \begin{pmatrix} \partial_x l_x \\ \partial_x l_y \\ \partial_y l_x \\ \partial_y l_y \end{pmatrix}, \quad (15)$$

and Onsager reciprocity imposes $\mathcal{D}_{l_{xy}}^{s_{yy}} = \mathcal{D}_{l_{yx}}^{s_{xy}}$ and $\mathcal{D}_{l_{xx}}^{s_{yy}} = \mathcal{D}_{l_{yy}}^{s_{xy}}$. Swapping efficiencies, $\eta_{l \rightarrow s}$ and $\eta_{s \rightarrow l}$, are defined similarly as above. From Fig. 4(c), it appears that although the spin-to-orbit swapping diffusiv-

ity (red) is larger than the orbit-to-spin swapping diffusivity (blue), the total efficiency of the orbital-to-spin swapping efficiency remains much larger due to the small orbital diffusivity [Fig. 4(d)]. In the context of spin-orbit torque², spin swapping, being of bulk^{24,34} or interfacial origin³⁵, is responsible for additional torque components in magnetic multilayers, depending on the transport regime (diffusive versus Knudsen regime). The large orbital swapping efficiencies reported here suggest that in systems displaying orbital torque, deviations from the conventional damping-like torque can be expected³⁴.

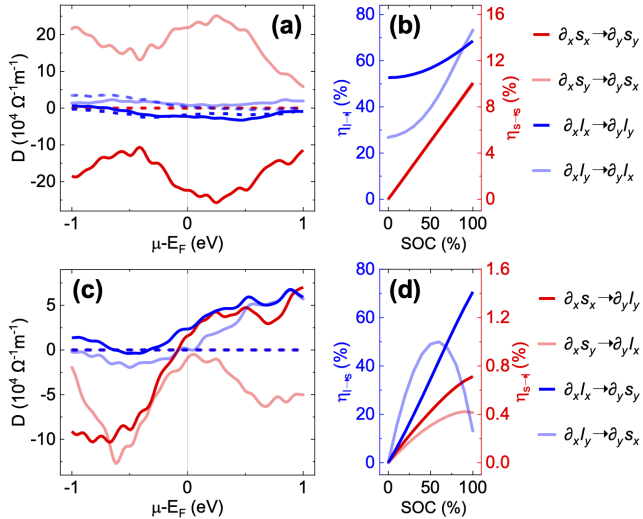


FIG. 4. (a) Spin (red), orbital (blue), and (c) spin-to-orbit (red) and orbit-to-spin (blue) swapping diffusivities as a function of the energy in tantalum, without (dashed lines) and with (solid lines) spin-orbit coupling. Corresponding (b) spin, orbit, and (d) spin-orbit swapping efficiencies as a function of the spin-orbit coupling. 100% corresponds to the full spin-orbit coupling strength of tantalum.

Conclusion - Advancing research in orbitronics requires a proper description of spin and orbital diffusion in metals. As stated previously, whereas the vast majority of theoretical studies to date focus on orbital and spin currents generated by electric currents, our theory allows us to compute the orbital and spin currents induced by diffusive gradients of angular momenta. It reveals that

although orbital currents do not experience "orbital-flip" *per se*, their diffusivity in metals is much weaker than that of spin currents. This result seems at odds with recent experiments suggesting a reasonably long orbital diffusion length in transition metals^{13,15–19,36}. In diffusive transport though, the (spin or orbital) diffusion length is related to the product between the (spin or orbital) diffusivity \mathcal{D} and the (spin or orbital) relaxation time τ_r , $\lambda \propto \sqrt{\mathcal{D}\tau_r}$. Therefore, to model the orbital diffusion length in transition metals, the present theory must be completed by a theory of orbital relaxation which remains an open question. Our theory also quantifies the spin-to-orbit and orbit-to-spin polarization, i.e., the ability for a spin (orbital) current to generate a longitudinal orbital (spin) current, and finds that the orbital-spin polarization is very efficient, potentially as efficient as conventional spin polarization in 3d magnets. Finally, we show that orbital currents are subject to angular moment swapping even in the absence of spin-orbit coupling and can be as large as spin swapping, and orbit-to-spin swapping is much more efficient than spin-to-orbit swapping due to the weak orbital diffusion coefficient.

ACKNOWLEDGMENTS

X.N. appreciates Yuhao Jiang's advice and assistance during the code development phase. X.N. was supported by the China Scholarship Council Program. W.Z. was supported by the National Key Research and Development Program of China (Grants No. 2022YFB4400200), the National Natural Science Foundation of China (Grant No. 92164206, No. 52121001, and No. 52261145694), and the New Cornerstone Science Foundation through the XPLORER PRIZE. A.P. was supported by the ANR ORION project, grant ANR-20-CE30-0022-01 of the French Agence Nationale de la Recherche, A. M. was supported by France 2030 government investment plan managed by the French National Research Agency under grant reference PEPR SPIN – [SPINTHEORY] ANR-22-EXSP-0009, and by the EIC Pathfinder OPEN grant 101129641 "OBELIX". K.-W. K. was supported by the KIST Institutional Program and the National Research Foundation (NRF) of Korea (RS-2024-00334933), and K.-J. L. was supported by the NRF (NRF-2022M3H4A1A04098811).

¹ T. Nan, D. C. Ralph, E. Y. Tsymbal, and A. Manchon, *APL Materials* **9**, 120401 (2021).

² A. Manchon, J. Zelezny, M. Miron, T. Jungwirth, J. Sinova, A. Thiaville, K. Garello, and P. Gambardella, *Review of Modern Physics* **91**, 035004 (2019).

³ E. Saitoh, M. Ueda, H. Miyajima, and G. Tatara, *Applied Physics Letters* **88**, 182509 (2006).

⁴ B. A. Bernevig, T. L. Hughes, and S. cheng Zhang, *Physical Review Letters* **95**, 066601 (2005).

⁵ H. Kontani, T. Tanaka, D. Hirashima, K. Yamada, and J. Inoue, *Physical Review Letters* **102**, 016601 (2009).

⁶ D. Go, D. Jo, C. Kim, and H. W. Lee, *Physical Review Letters* **121**, 086602 (2018).

⁷ D. Go, J. philipp Hanke, P. M. Buhl, F. Freimuth, G. Bihlmayer, H. woo Lee, Y. Mokrousov, and S. Blügel, *Scientific Reports* **7**, 46742 (2017).

⁸ T. Yoda, T. Yokoyama, and S. Murakami, *Nano Letters* **18**, 916 (2018).

⁹ A. E. Hamdi, J. Y. Chauleau, M. Boselli, C. Thibault, C. Gorini, A. Smogunov, C. Barreteau, S. Gariglio, J. M. Triscone, and M. Viret, *Nature Physics* (2023), 10.1038/s41567-023-02121-4.

¹⁰ D. Go and H. woo Lee, *Physical Review Research* **2**, 13177 (2020).

¹¹ S. Ding, A. Ross, D. Go, L. Baldrati, Z. Ren, F. Freimuth, S. Becker, F. Kammerbauer, J. Yang, G. Jakob, Y. Mokrousov, and M. Kläui, *Physical Review Letters* **125**, 177201 (2020).

¹² D. Lee, D. Go, H. J. Park, W. Jeong, H. W. Ko, D. Yun, D. Jo, S. Lee, G. Go, J. H. Oh, K. J. Kim, B. G. Park, B. C. Min, H. C. Koo, H. W. Lee, O. J. Lee, and K. J. Lee, *Nature Communications* **12**, 6710 (2021).

¹³ D. Go, D. Jo, K.-W. Kim, S. Lee, M.-G. Kang, B.-G. Park, S. Blügel, H.-W. Lee, and Y. Mokrousov, *Physical Review Letters* **130** (2023), 10.1103/physrevlett.130.246701.

¹⁴ S. Ding, Z. Liang, D. Go, C. Yun, M. Xue, Z. Liu, S. Becker, W. Yang, H. Du, C. Wang, Y. Yang, G. Jakob, M. Kläui, Y. Mokrousov, and J. Yang, *Physical Review Letters* **128**, 067201 (2022).

¹⁵ G. Sala and P. Gambardella, *Physical Review Research* **4** (2022), 10.1103/PhysRevResearch.4.033037.

¹⁶ H. Hayashi, D. Jo, D. Go, T. Gao, S. Haku, Y. Mokrousov, H. W. Lee, and K. Ando, *Communications Physics* **6** (2023), 10.1038/s42005-023-01139-7.

¹⁷ R. Fukunaga, S. Haku, H. Hayashi, and K. Ando, *Physical Review Research* **5** (2023), 10.1103/PhysRevResearch.5.023054.

¹⁸ I. Lyalin, S. Alikhah, M. Berritta, P. M. Oppeneer, and R. K. Kawakami, (2023).

¹⁹ Y.-G. Choi, D. Jo, K.-H. Ko, D. Go, K.-H. Kim, H. G. Park, C. Kim, B.-C. Min, G.-M. Choi, and H.-W. Lee, *Nature* **619**, 52 (2023).

²⁰ S. Han, H.-W. Lee, and K.-W. Kim, *Physical Review Letters* **128**, 176601 (2022).

²¹ S. Bhowal and G. Vignale, *Physical Review B* **103**, 195309 (2021).

²² T. P. Cysne, S. Bhowal, G. Vignale, and T. G. Rappoport, *Physical Review B* **105**, 195421 (2022).

²³ A. Pezo, D. G. Ovalle, and A. Manchon, *Physical Review B* **106**, 104414 (2022).

²⁴ M. B. Lifshits and M. I. Dyakonov, *Physical Review Letters* **103**, 186601 (2009).

²⁵ S. Rammer and H. Smith, *Reviews of Modern Physics* **58**, 323 (1986).

²⁶ “Supplemental materials.”.

²⁷ J. Sinova, D. Culcer, Q. Niu, N. A. Sinitsyn, T. Jungwirth, and A. H. MacDonald, *Physical Review Letters* **92**, 126603 (2004).

²⁸ V. Bonbien and A. Manchon, *Physical Review B* **102**, 085113 (2020).

²⁹ H.-J. Park, H.-W. Ko, G. Go, J. H. Oh, K.-W. Kim, and K.-J. Lee, *Physical Review Letters* **129**, 37202 (2022).

³⁰ J. C. Slater and G. F. Koster, *Physical Review* **94**, 1498 (1954).

³¹ D. A. Papaconstantopoulos, *Handbook of the Band Structure of Elemental Solids*, second edi ed. (Springer, New York, 2015) p. 410.

³² M. D. Jaffe and J. Singh, *Solid State Communications* **62**, 399 (1987).

³³ D. Dai, H. Xiang, and M. H. Whangbo, *Journal of Computational Chemistry* **29**, 2187 (2008).

³⁴ H. Saidaoui and A. Manchon, *Physical Review Letters* **117**, 036601 (2016).

³⁵ S. H. C. Baek, V. P. Amin, Y. W. Oh, G. Go, S. J. Lee, G. H. Lee, K. J. Kim, M. D. Stiles, B. G. Park, and K. J. Lee, *Nature Materials* **17**, 509 (2018).

³⁶ S. Lee, M. G. Kang, D. Go, D. Kim, J. H. Kang, T. Lee, G. H. Lee, J. Kang, N. J. Lee, Y. Mokrousov, S. Kim, K. J. Kim, K. J. Lee, and B. G. Park, *Communications Physics* **4**, 234 (2021).